# Comparison of measured static and quasi-static deflections of industrial manipulators

Nikolas Alexander Theissen, Monica Katherine Gonzalez, Theodoros Laspas, and Andreas Archenti
*KTH Royal Institute of Technology, Sweden*

## Abstract

This work presents a comparison of the measured static and quasi-static deflections of industrial manipulators. For the measurement of the static deflections, the manipulator remains in static positions while for the quasi-static deflections the manipulator follows a circular trajectory. The static deflections are measured at discretised static configurations along circular trajectories while the quasi-static deflections are measured under circular motion along the same trajectories. Loads of different magnitudes were induced with the Loaded Double Ball Bar (LDBB). The static and quasi-static displacements are measured using a (Linear Variable Differential Transformer) LVDT embedded in the Loaded Double Ball Bar and a Leica AT901 laser tracker. These measurement procedures are implemented in a case study on a large-sized serial articulated industrial manipulator from ABB in three different positions of its workspace. The presented method shows that the measured quasi-static deflections are on average approximately 22% bigger than the measured static deflections. The quasi-static deflections are at most 32% bigger than the static deflections. Finally, the manuscript concludes with a discussion on how the measurement procedure could be used to analyse the difference between using the static stiffness and the apparent quasi-static stiffness of an industrial manipulator for trajectory optimisation.

## 1. Introduction

The demand for industrial robots has been increasing and can be considered significant, as shown by the market volume of approximately 16.2 billion USD achieved by these products in 2017 [1]. Industrial robots are capable of realizing numerous tasks while at the same time providing modern manufacturing environments with the flexibility to adapt to smaller lot sizes. Additionally, they are cheaper based on price per unit of working space when compared with specialized machinery, e.g., milling machines, lathes, or machining centres.

These capabilities have led to the integration of industrial robots across important industries for a wide variety of commodities such as consumer electronics, industrial machinery, or vehicles and in a variety of applications ever since 1961. For industrial manipulators in conventional metal cutting, stiffness is an informative performance criterion. It is even more important than in machine tools as machine tool tend to be significantly stiffer, i.e. optimising the process parameters more easily yield products of the required Geometric Dimensions and Tolerances (GD&T). The stiffness of a mechanical system can be defined as its capacity to sustain loads, which result in a change of its geometry [4]. One differentiates between static, quasi-static, and dynamic stiffness. This work investigates the difference between static stiffness, i.e. static manipulator, and quasi-static stiffness, i.e. moving manipulator. It is possible that to measure the static and quasi-static stiffness of an industrial manipulator most accurately one should not move the system. From a theory point of view, one can exert static loads, i.e. the frequency is equal to 0 Hz, and the quasi-static loads, i.e. the frequency is greater than 0 Hz and lower than 0.5 Hz, for the identification without moving the industrial manipulator [2]. However, this work follows the idea outlined by Archenti and Nicolescu [3] that to accurately identify a system's capability for an intended task, one should emulate the intended task. Case studies on machine tools, see Laspas et al. [4] and Theissen et al. [5], have implied that there can be differences in the magnitude of the static and quasi-static stiffness. This work quantifies this difference for a single large-sized serial articulated manipulator.

## 2. Methodology

This section describes the measurement devices, measurement procedures, and data processing for the measurement and identification of the static and quasi-static deflections. The static and quasi-static procedures use the same measurement devices but differ in the measurement procedure and the data analysis. The quasi-static procedure builds on the static procedure.

### 2.1. Measurement devices

The conceptual measurement setup can be seen in Figure 1. The setup comprises the following equipment: 1) a large-sized serial articulated industrial robot with its corresponding controller (not included in the picture), 2) a Leica AT901-LR laser tracker (not included in the picture) [6] with a 0.5 '' Red Ring Reflector (RRR), 3) the measurement instrument Loaded Double Ball Bar (LDBB) [7] with a DTA-3G8-3-CA LVDT [8], 4) a rigid Table Link (TL), and 5) a dummy end-effector with Tool Centre Point (TCP) and a mechanical interface for the Spherically Mounted Retro-reflector (SMR). The deflection measurements are performed with two different metrology loops. The first metrology loop uses an LVDT for the deflection measurement, the second loop uses the laser tracker.

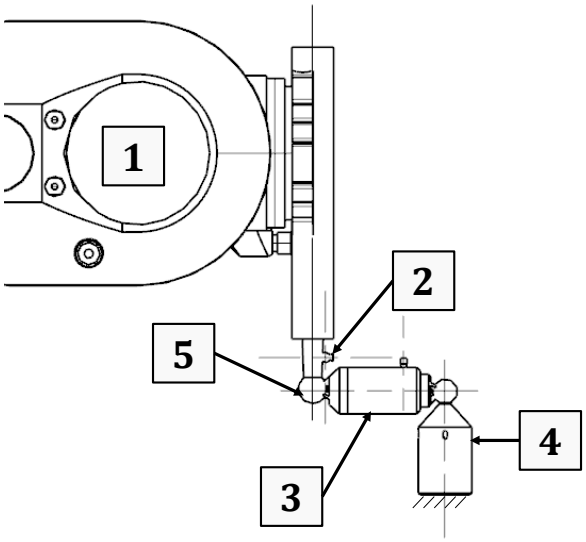


Figure 1: Measurement setup

### 2.2. Measurement process

The static measurement induces loads of 125 N, 250 N, 375 N, and 500 N at 37 indexed positions along a circular trajectory, see Figure 2. Target 1 and 37 are at the same position, i.e. the static circle has the same start and endpoint. Once the manipulator reaches a stable position the static loads are induced at the TCP. Once the LDBB reaches a stable load level, i.e. within a limit of $\pm 0.7\%$ at 125 N down to $\pm 0.2\%$ at 500 N, the measurements are acquired with both the laser tracker, using the *Precise* measurement profile, and the LVDT, using continuous data recording at 1000 Hz. The quasi-static measurement procedure induces loads of 125 N, 250 N, 375 N, and 500 N along the circular trajectory with a diameter of approximately 250 mm. In this case, the manipulator executes a trigger movement by moving 1 mm up and down at the start point of the circle, with a velocity of 250 mm/sec. Then the manipulator moves two times clockwise about the same circular trajectory, see Figure 2. The circles were measured with an Angular Overshoot (AOS) of 180° to exclude transient effects from the measurement data [20]. The manipulator followed the trajectory with a Cartesian velocity of 50 mm/sec. At this velocity, dynamic effects can be assumed negligible. Both the laser tracker and the LVDT are set to continuous data recording at 1000 Hz, this dissected the circle into approximately 16,000 measurement points. For both the static and the quasi-static measurement multiple force components were exerted simultaneously. This approach differs from the description of circular testing according to ISO 230-4 [9]. Thus, the Z-axis component's magnitude was chosen to be roughly 1/3 of the total load, while the remaining 2/3 were split between the X- and Y-axis components, whose contribution depended on the position of the LDBB along the circle.

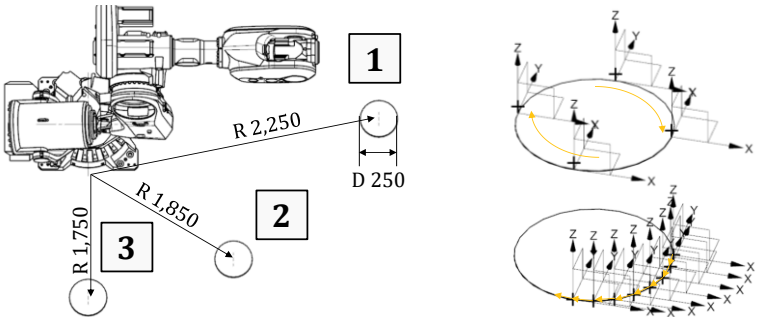


Figure 2: Positions of circles 1.-3. in the robot's base coordinate system (left) and the targets along the circle for the static (right down) and quasi-static measurement (right up). The targets along the circle for the static measurement are exemplified for the first quadrant.

The procedure for both the static and quasi-static measurement is repeated at three positions numbered as Circle 1 to Circle 3 and have different distance R from Robot's Base Coordinate System (RBCS) origin (see Figure 2) maintaining the same Z height from the RBCS origin.

### 2.3. Data analysis

The deflections $\Delta X$ are calculated as the position difference of the loaded TCP position $X_{i,j}$, i.e. for the positions $i$ and the loads $j = [250\,N, 375\,N, 500\,N]$, and the reference TCP position $X_{i,ref}$ at a load of 125 N according to:

$$\Delta X_{i,j} = \begin{bmatrix} \delta x \\ \delta y \\ \delta z \end{bmatrix}_{i,j} = \begin{bmatrix} x \\ y \\ z \end{bmatrix}_{i,j} - \begin{bmatrix} x \\ y \\ z \end{bmatrix}_{i,ref} \quad (1)$$

The magnitude of the deflection $\left\|\Delta X_{i,j}\right\|_2$, which is referenced in the subsequent section, is calculated as the Euclidean norm of the deflection:

$$\left\|\Delta X_{i,j}\right\|_2 = \sqrt{\delta x^2 + \delta y^2 + \delta z^2} \quad (2)$$

Thus, the magnitude of the deflection corresponds to the distance between the loaded and unloaded position. For the static deflections at the $i = [1, \dots, 37]$ TCP positions this calculation is straight forward for the measurement data from both, the laser tracker and the LVDT. For the quasi-static deflections at the $i = [1, \dots, 15899]$ TCP positions, first, the AOS needs to be removed then the difference can be calculated. In both, the static and quasi-static case, the measurement from the LVDT needs to be compensated for the deflection of the table link. All deflections are calculated relative to a reference load of 125 N, this removes the influence of the hysteresis in the setup. In the following section, the wording *acting load* is used to highlight this idea. An acting load of 125 N means that the system is loaded with 250 N, but the difference with respect to 125 N is considered.

## 3. Results

The magnitude of the static and quasi-static deflections along Circle 1 for acting loads of 125 N, 250 N, and 375 N can be seen in Figure 3 and Figure 4. Circle 1 Is positioned about 2.250 m from origin. The magnitude of the deflection, as one would expect, increases with the load but also changes along the circular trajectory as the Cartesian stiffness of the industrial manipulator depends on the configuration [10]. The data have been measured using the LVDT as well as a laser tracker. The average differences the static and quasi-static deflection between the LVDT and the laser tracker equal around 40 µm. Figure 3 and Figure 4 support the observation that both measurement instruments yield results close to a couple of tenth of micrometres. This differences can be accounted for by the uncertainty of the laser tracker, around 10 µm, as well as the different measurement position, the distance between both measurement points equals approximately 6 mm. The remaining difference of about 30 µm could be explained by an angular error of around 0.3 degrees. This observation is supported by the magnitude of the measured static and quasi-static deflections for Circle 1. to Circle 3. in Table 1 to Table 3. Furthermore, the tables show that the magnitude of the deflections increases with the distance from joint 1, i.e. the origin of the RBCS.

For all acting loads and all circles in the case study, the quasi-static deflections are bigger than the static deflections. The static and quasi-static deflections are very similar in their characteristics but differ in their magnitudes. The measured quasi-static deflections are on average approximately 22% bigger than the measured static deflections. The quasi-static deflections are at most 32% bigger than the static deflections.

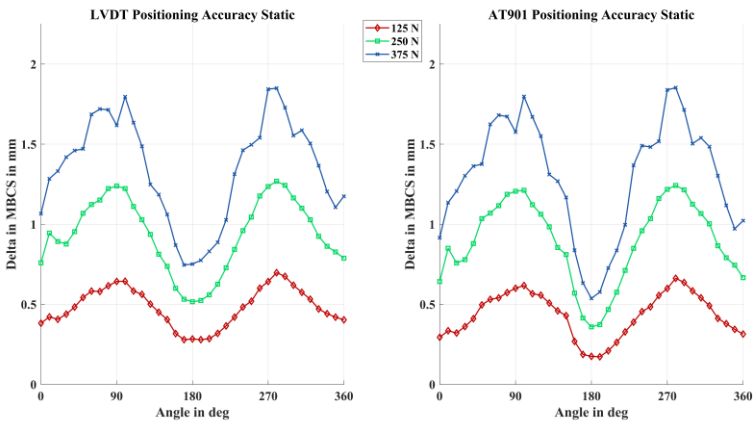


Figure 3: Magnitude of the static difference, i.e. Euclidean norm of the Cartesian deflections, as measured by the LVDT (left) and AT901 laser tracker (right).

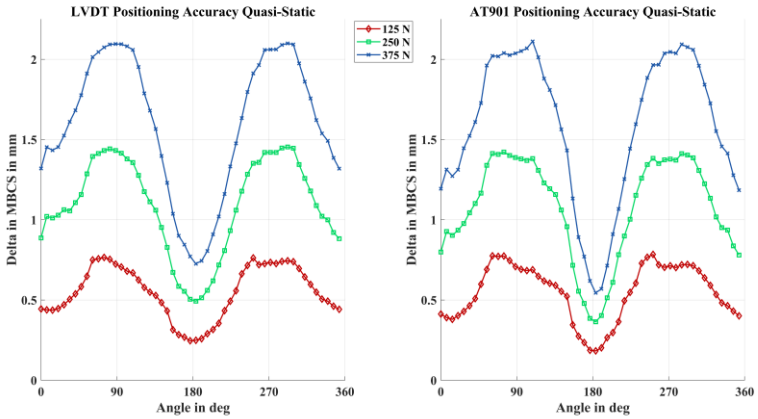


Figure 4: Magnitude of the quasi-static difference, i.e. Euclidean norm of the Cartesian deflections, as measured by the LVDT (left) and AT901 laser tracker (right).

## 4. Discussions

The results displayed in Table 1 to Table 3 imply that there can be significant differences in the magnitude of the static and quasi-static deflections. It needs to be pointed out that there is no apparent determinism that leads to the observed difference, i.e. from the observations of this case study one cannot derive useful information about other serial articulated manipulators. One cannot even derive further information about the remaining workspace for the investigated industrial manipulator. Further investigations require the analysis of the influence of Cartesian velocities, i.e. friction, as well as different controller settings in terms of operation mode and task program on the difference between static and quasi-static deflections. Nevertheless, the case study shows that the LDBB is capable of accurately identifying the deflections of industrial manipulators along circular trajectories. This may facilitate a pragmatic compliance calibration of industrial manipulators. The pragmatism in that sense lies in the possibility to calibrate an industrial manipulator task-dependent, i.e. in the relevant portion of the workspace with loads in the magnitude of the task. This may make compliance calibration cheaper, faster, and potentially more accurate.

## 5. Acknowledgement

The authors would like to thank VINNOVA and the SMART advanced manufacturing cluster for funding this research as a part of the COMACH project (Grant Agreement ID: S0120). The authors would like to also express
their gratitude to the Centre for Design and Management of Manufacturing Systems (DMMS) for their financial support.

Table 1: Magnitude of the measured static and quasi-static deflections along circle 1. Average of the norm of Cartesian deflections Circle 1 (Distance 2.250 m).

| | Static (S) | | Quasi-Static (QS) | | |
|---|---|---|---|---|---|
| Acting Load in N | LVDT in mm | AT901 in mm | LVDT in mm | AT901 in mm | QS/S |
| 125 | 0.48 | 0.43 | 0.55 | 0.55 | +20 % |
| 250 | 0.94 | 0.89 | 1.10 | 1.10 | +18 % |
| 375 | 1.35 | 1.30 | 1.62 | 1.62 | +20 % |

Table 2: Magnitude of the measured static and quasi-static deflections along circle 2. Average of the norm of Cartesian deflections Circle 2 (Distance 1.850 m).

| | Static (S) | | Quasi-Static (QS) | | |
|---|---|---|---|---|---|
| Acting Load in N | LVDT in mm | AT901 in mm | LVDT in mm | AT901 in mm | QS/S |
| 125 | 0.22 | 0.24 | 0.25 | 0.32 | +25 % |
| 250 | 0.45 | 0.44 | 0.55 | 0.62 | +32 % |
| 375 | 0.69 | 0.62 | 0.74 | 0.90 | +25 % |

Table 3: Magnitude of the measured static and quasi-static deflections along circle 3. Average of the norm of Cartesian deflections Circle 3 (Distance 1.750 m)

| | Static (S) | | Quasi-Static (QS) | | |
|---|---|---|---|---|---|
| Acting Load in N | LVDT in mm | AT901 in mm | LVDT in mm | AT901 in mm | QS/S |
| 125 | 0.14 | 0.15 | 0.17 | 0.20 | +28 % |
| 250 | 0.30 | 0.30 | 0.32 | 0.38 | +17 % |
| 375 | 0.45 | 0.44 | 0.47 | 0.56 | +16 % |

## 6. References


[1] INTERNATIONAL FEDERATION OF ROBOTICS. *Executive Summary World Robotics 2018 Service Robots*, 2018.

[2] Rivin E I. *Handbook on stiffness & damping in mechanical design.* New York: ASME Press, 2010. ISBN 0791802930.

[3] Archenti Aand Nicolescu M. Accuracy analysis of machine tools using Elastically Linked Systems [online]. *CIRP Annals - Manufacturing Technology*, 2013, 62(1), 503-506. ISSN 00078506. Available under: doi:10.1016/j.cirp.2013.03.100

[4] Laspas T, Theissen Nand Archenti A. Novel methodology for the measurement and identification for quasi-static stiffness of five-axis machine tools [online]. *Precision Engineering*, 2020, 65, 164-170. ISSN 01416359. Available under: doi:10.1016/j.precisioneng.2020.06.006

[5] Theissen N, Laspas T, Szipka Kand Archenti A *Measurement and identification of translational stiffness matrix for static loads in machine tools. In: Virtual International Conference 2020*, 2020.

[6] LEICA GEOSYSTEMS. *User Manual AbsoluteTracker AT901*.

[7] Archenti, A., Hg. *A Computational Framework for Control of Machining System Capability. From Formulation to Implementation.* Stockholm, 2011. ISBN 978-91-7501-162-2.

[8] MIRCO-EPSILON USA. *Linear inductive displacement sensors*.

[9] International Organization for Standardization, *ISO 230-4:2005 Test code for machine tools – Part 4: Circular tests for numerically controlled machine tools*.

[10] Klimchik A, Furet B, Caro Sand Pashkevich A. Identification of the manipulator stiffness model parameters in industrial environment [online]. *Mechanism and Machine Theory*, 2015, 90, 1-22. ISSN 0094114X. Available under: doi:10.1016/j.mechmachtheory.2015.03.002